Lecture Session (LeS): E.14 Source zone treatment

DOMINATING PROCESSES DURING DNAPL REMOVAL FROM THE SATURATED ZONE USING THERMAL WELLS

Uwe Hiester, Martina Müller, Oliver Trötschler, Hans-Peter Koschitzky, *VEGAS* – Research Facility for Subsurface Remediation, Universität Stuttgart, Germany

Ralph S. Baker, John LaChance and Gorm Heron, TerraTherm, Inc., Fitchburg, Massachusetts, USA

Myron Kuhlman, MK Tech Solutions Inc., Houston, Texas, USA

Corresponding author: Uwe Hiester, *VEGAS*, Universität Stuttgart, Pfaffenwaldring 61, 70569 Stuttgart, Germany, phone: +49 (0)711 685-64745, uwe.hiester@iws.uni-stuttgart.de

Keywords: Contaminated soil, chlorinated solvents, source remediation, low permeable soil layer, in situ thermal remediation, Thermal Conduction Heating (TCH), heat transport

INTRODUCTION

Dense Non-Aqueous Phase Liquid (DNAPL) source zones are considered to be among one of the most complex and difficult types of contaminated sites to remediate. To remove the contaminated source zone, conventional clean-up methods like 'pump and treat' often fail or are insufficient due to low mass removal rates and remaining NAPL pools. Soil vapour extraction (SVE), multiphase extraction, in-situ air sparging, chemical oxidation, surfactant flushing and steam-air injection are all challenged by heterogeneity. The heterogeneities are primarily characterized by a large variation of hydraulic conductivity and/or by layers of low permeability within the source volume to be remediated. Since contaminants are entrapped in both high and low permeable layers, preferential flow and bypassing of lower permeable zones can leave such residual contamination widely untreated [HIESTER ET AL., 2007].

In-Situ Thermal Remediation (ISTR) technologies including Steam-Enhanced Remediation (SER), Electrical Resistance Heating (ERH) and Thermal Conduction Heating (TCH) are beginning to be widely applied to overcome these limitations. While SER has its greatest applicability to higher permeable zones in the unsaturated zone and also beneath the water table, ERH and TCH are most often applied within low and moderate permeability zones. ERH depends on the electrical conductivity of soil, which varies over a factor of several orders of magnitude depending on soil type, from clay to sand. High electrical conductivity is associated with zones that retain water and contain clay minerals. Furthermore ERH is limited to achieving the boiling point of water, similar to SER. By contrast TCH (also known as In-Situ Thermal Desorption or ISTD) is governed by the thermal conductivity of soil which is one of the most invariant of all soil physical properties, varying only by a factor of about three over a wide range of soil types from clay to gravel. Mainly by conductive heating, TCH can heat the subsurface to temperatures below, at or if needed well above the boiling point of water in a dry soil. Additionally, density driven hot water flow (affecting only the liquid phases) [LI, 2004] and capillary forces in a heat pipe system (affecting both liquid and gaseous phases) enable a convective heat transport even in low permeability soils [UDELL & FITCH, 1985]. Thus TCH has applications in layers of low permeability, heterogeneous subsurface settings and for contaminants with moderate to high boiling points.

MOTIVATION AND SCOPE OF RESEARCH WORK

Recognizing the need to gain a better understanding of the underlying mechanisms of TCH/ISTD for treatment of DNAPL in the saturated zone, *VEGAS* (physical experiments on different scales), MK Tech Solutions (numerical simulations) and TerraTherm (coordinator) formed a research collaboration. This research project was intended to rigorously investigate and help optimise these processes and accompanying contaminant mobilization and removal. The project was funded by the U.S. Strategic Environmental Research and Development Program (SERDP).

The results from initial bench-scale two-dimensional (2-D) remediation experiments are the subject of a companion paper [BAKER ET AL. 2008]. 2-D experiments had been used to study the principal mechanisms

that control the performance of TCH/ISTD below the water table. The results served as a benchmark for the numerical simulations allowing testing of its reliability for representing such processes. The experimental data thus enabled calibration of the numerical model to improve the accuracy of subsequent simulations. The calibrated numerical model was then used to design the more complicated experiments, including 3-D experiments conducted in two large-scale tanks. The objectives of the overall project are:

1) to determine the impact of boundary conditions like soil permeability or groundwater flux on the heated zone,
2) to determine the relative significance of the various contaminant removal mechanisms below the water table (e.g. volatilization, stream stripping),
3) to assess the percentage of the DNAPL source removal and accompanying change in water saturation at various treatment temperatures/durations through boiling; and
4) to evaluate the potential for DNAPL mobilization, either through volatilization and recondensation (gaseous and liquid phase), and/or pool mobilization (only liquid phase) outside of the target treatment zone (TTZ) during heating.

SET-UP OF 3-D EXPERIMENTS

For the 3-D experiments carried out at *VEGAS*, two adjacent stainless steel tanks with a base of 3 m x 6 m and 6 m x 6 m had each been filled with soil up to a height of 4.5 m (75 m^3 and 150 m^3). A 1.5 m high layer of lower permeability in the middle of each tank (i.e. an aquitard) was positioned between an overlying vadose zone layer and an underlying aquifer layer, both of higher permeability. The set-up of the smaller tank is shown in Figure 1 and tank specific data are summarized for both tanks in Table 1. In each tank, four heater (or if desired, eight) wells could be operated. They were arrayed in a square, 1 m x 1 m pattern. The groundwater level at the outflow was controlled so as to maintain a constant head boundary at 3 m above base at the top of the aquitard layer, but groundwater inflow varied depending on the experimental phase.

Each tank was equipped with Pt100 temperature sensors in 12 layers with 15 to 17 sensors/layer (approx. 200 sensors/tank). The temperature sensors were arranged in a V-shape between the inflow and the centre of the container (Figure 1 Top: A-Z in blue colour). Additionally, high-temperature and corrosion-resistant Time Domain Reflectory (TDR) sensors were installed to measure the water saturation along the tank centre line (Figure 1: profile A-F in pink colour (left-hand side).

For the remediation experiments, DNAPL pools could be created by injecting a known substance into two NAPL-storage lenses. These lenses were located within the aquitard in a height of 2.7 - 2.9 m (upper lens) and of 2.0 - 2.2 m (bottom lens) (Fig. 1, bottom: shaded in red) above base (a.b.) To monitor a potential contaminant migration during the remediation experiments, sampling ports were integrated into the set-up of both tanks at 7 different heights with 3 to 25 ports on each level. An initial focus of the research was on a potential risk of downward migration of DNAPL into the underlying aquifer, where most of the sampling ports were installed.

To identify the operational parameters of major interest, numerical simulations were performed. The migration of a steam front within the saturated zone results from a complex combination of effects, most notably convective spreading in all directions, the heat-pipe effect [UDELL & FITCH, 1985] and steam override. The results of the numerical simulations showed that under the conditions being considered, two characteristic types of steam front migration have to be differentiated. In the case of a ‘sufficient’ cooling at the bottom of the aquitard as by a moderate or high flux of groundwater in the aquifer, the steam front remains in the aquitard (steam front type 1). In contrast to this, low or even no groundwater flux might enable a steam front to migrate into the lower aquifer (steam front type 2). Figure 2 shows schematically these two different steam front propagation scenarios. Since a steam front generated from conductive heating of the DNAPL storage lenses will contain high concentrations of contaminants and might displace recondensed and accumulated liquid contaminants in various directions, a type-2 steam front would be expected to cause an irreversible transport of contaminants into the aquifer. In relation to the tank set-up, a contaminant recovery by SVE would be impossible given the positions of the heating and extraction wells under consideration.

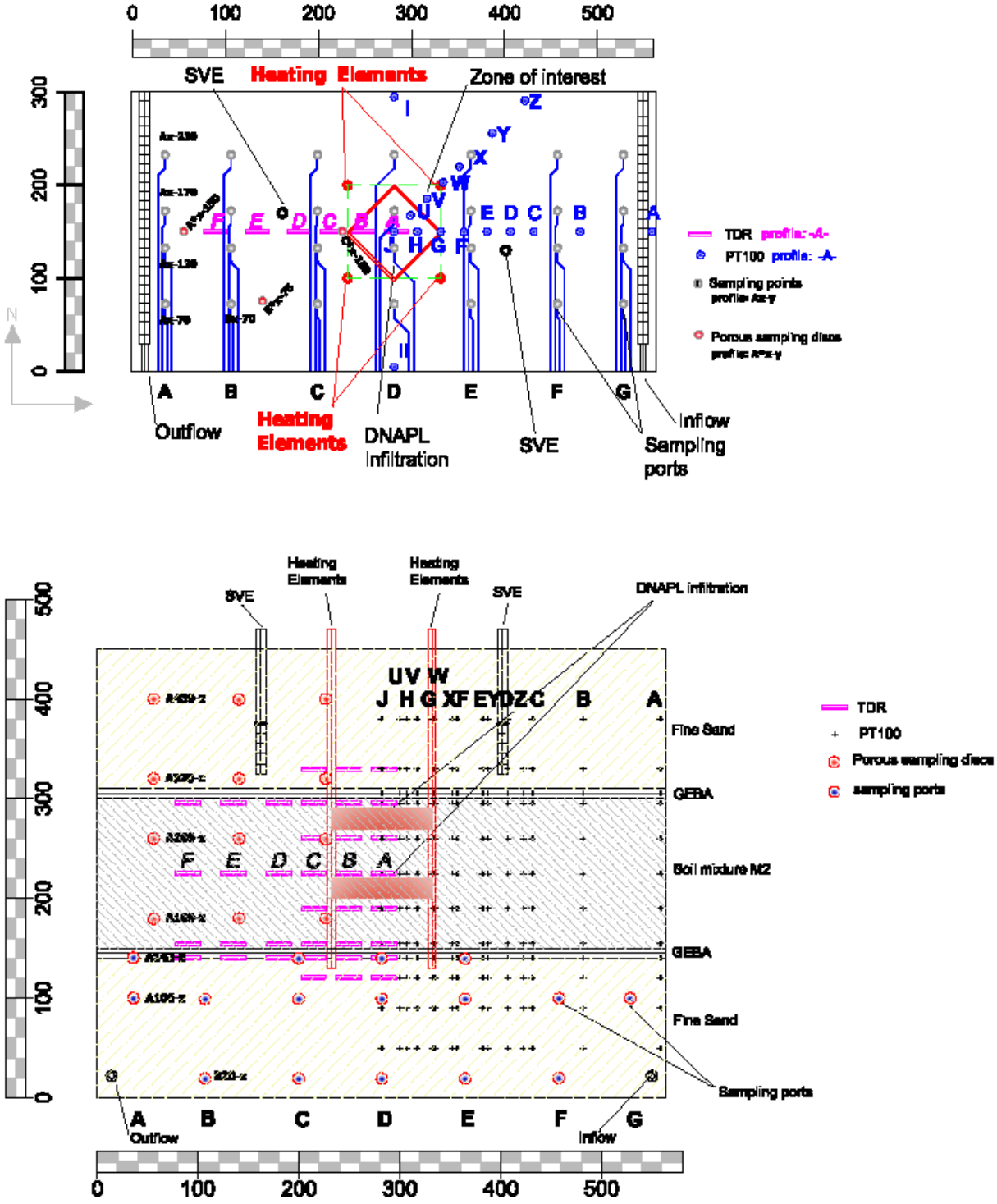

FIGURE 1: Set-up of the smaller 3-D tank. Top: Plan view; bottom: side view.

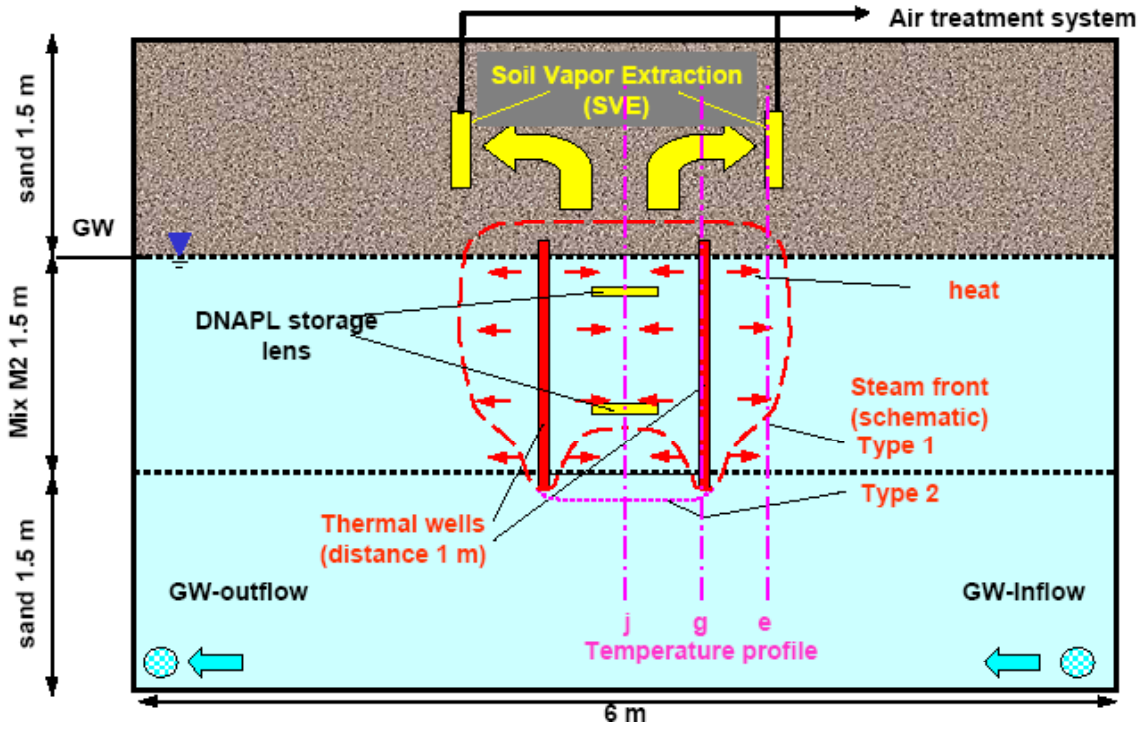

FIGURE 2. Schematic steam front propagation based on numerical simulations (side view).

To quantify the impact of the groundwater influx on the temperature distribution and steam front propagation, one heat transport experiment was conducted in each tank while varying the groundwater flux. The thermal wells operated at full power (6kW) and the groundwater outflow was kept constant at a height of 3 m a.b. The operational settings are summarized in Table 1.

TABLE 1: Summarized Data from both Tanks.

	Large Container	Small Container
Length **Width** **Height**	6 m 6 m 4.5 m	6 m 3 m 4.5 m
K_S of lower permeability soil layer	1 to 3 x 10^{-6} m/s	1 to 4 x 10^{-7} m/s
K_S of higher permeability soil layers	1 x 10^{-3} m/s	1 x 10^{-4} m/s
Power of heater array	6 kW (4 heaters)	6 kW (4 heaters)
Groundwater outflow (const. head)	3 m above base	3 m above base
Phase 1a	333.3 l / (tank width x day)	333.3 l / (tank width x day)
Phase 1b	166.7 l / (tank width x day)	223.3 l / (tank width x day)
Phase 1c	48.3 l / (tank width x day)	166.7 l / (tank width x day)
Phase 1d	1.7 l / (tank width x day)	10 l / (tank width x day)
Phase 1e	---	666.7 l / (tank width x day)
Phase 1f	---	1333.3 l / (tank width x day)

RESULTS

The following results focus on the heat transport experiments and the interpretation of the temperature distribution. The temperature data are used to interpret the steam front migration.

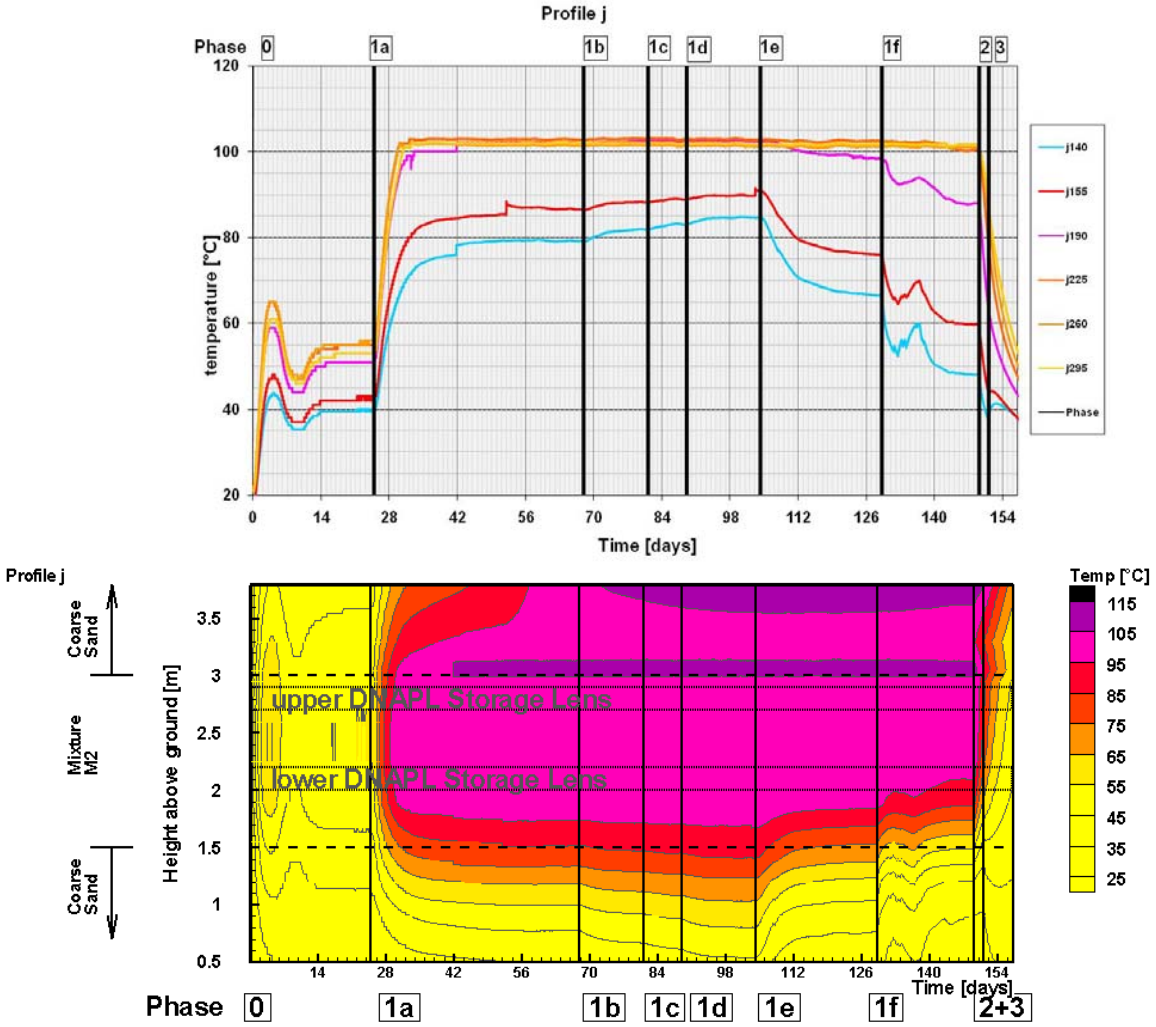

FIGURE 3. Temperature development in the central profile j, located equidistant from the heaters. Top: time-variation curves; bottom: spatial interpolation of the measured data.

The development of the temperatures at the central profile “j” over the course of the heat transport experiment in the smaller tank is shown in Figure 3 as an example. Both diagrams present the same data. However, the lower diagram also shows the spatial interpolation of the temperatures. We shall focus on the variation of the groundwater influx during the phases 1a – 1f (see Table 1). The experimental settings and the results during the preliminary low-power phase 0 and the final cool-down phases 2 and 3 are beyond the scope of this paper.

Independent of the groundwater flux during phase 1, the temperatures reached above 100°C in the upper NAPL storage lens. The steam front swept the upper DNAPL storage lens. Thus, no influence of the groundwater influx on the temperatures in the upper part of the aquitard was observed.

In contrast to this, under the present heater configuration, the temperatures in the lower NAPL storage lens were dominated by the change in groundwater flux. For higher groundwater discharges (phases 1e and 1f), temperatures decreased and the steam front collapsed in the lower lens.

Numerical simulations indicated a breakthrough of the steam front into the lower aquifer under the no-flow conditions. This was not observed in the experiment for no-flow conditions (phase 1d). The simulations generally tracked the characteristics of the temperature distribution at earlier times. Dependent on the hydrostatic pressure $\rho_{water} \cdot g \cdot \Delta h$ of the groundwater, the pressure associated with the boiling of water $p_{boiling}$ increases in the saturated zone by depth:

$$p_{boiling} = p_{atm} + \rho_{water} \cdot g \cdot \Delta h \quad (1)$$

where: p_{boilng} = pressure at which water boils
p_{atm} = atmospheric pressure
ρ_{water} = density of water
g = gravity constant
Δh = height of the saturated zone at the evaluated point

Therefore the boiling temperature $T_{boiling}$ to produce steam from the water in the saturated zone increases, according to WAGNER [1973]:

$$\ln p_{boiling,r} = \frac{a\tau + b\tau^{1.5} + c\tau^3 + d\tau^6}{T_r} \quad (2)$$

where: $p_{boiling,r}$ = $p_{boiling}/p_c$ = reduced pressure
(pressure at which water boils / pressure at critical point)
T_r = $T_{boiling}/T_c$ reduced temperature
(Temperature at which water boils / Temperature at critical point)
τ = $1-T_r$

The existence of steam at 1.5 m below the groundwater table (1.5 m a.b.) is related to a temperature of nearly 104°C. During the heat transport experiment the steady state temperatures at the bottom of the aquitard did not exceed 95°C indicating the lack of steam and the capability to steam water at this depth. Therefore only a one-phase system (i.e., warm / hot water) exists at the bottom of the lower permeability layer and in the coarse sand aquifer.

Nevertheless, steady state temperatures of the at the top of the aquitard correlated well with the specific groundwater flow [m^3/(tank width*d)] as shown in Figure 4. The data at the central profile "j" between the heaters of both heat transport experiments are illustrated. With increasing groundwater flux the temperatures decreased due to the increasing energy output of the groundwater discharge. The polynomial correlations between temperature and groundwater flux (3rd order for the small tank, 2nd order for the large tank) show correlation coefficients $R^2 > 0.99$. For higher discharges an asymptotic characteristic of the correlation was found. Due to the limited convective heat transfer coefficient across the boundary between the lower and higher permeability zones, temperature decreased more slowly with higher groundwater flux. At a certain discharge, the energy lost with the groundwater outflow achieved a maximum.

Although the soil permeability within the two tanks differed by one order of magnitude (Table 1), only minor temperature differences could be observed between the tanks within the lower part of the layer of lower permeability (Figure 4, 155 and 190 cm a.b.) .This is because convection and convection are both high between the heaters, i.e., numerical simulations show that energy transfer by convection is as high as energy transfer by conduction in the low-permeability soil between the heaters during most of the experiment. Within the permeable aquifer (Figure 4, 140 cm a.b.), the advective heat transport is always equal to the conductive heat transfer rate. In both structures, aquitard as well as aquifer, higher temperatures were observed in the layers with lower permeability, within which the heaters were primarily positioned. Here, the conductive heat transport could be more important compared to advective heat transport early in the experiment. Similar correlations were observed for other profiles but the temperatures were not as high as in the central profile "j".

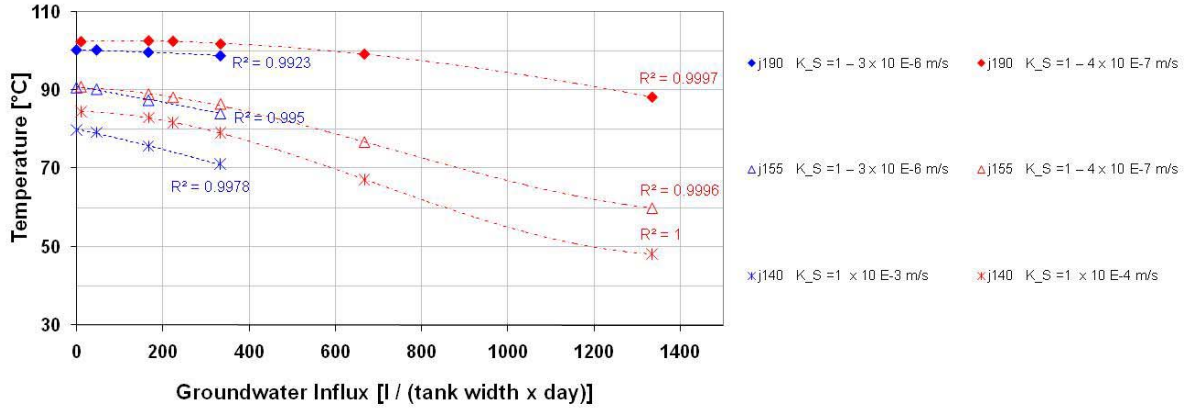

FIGURE 4: Correlation between groundwater flux and steady state temperatures during the experimental phases observed at the central profile "j" at 155 and 190 cm a.b. within the lower permeability layer, and 140 cm a.b. within the underlying aquifer.

In contrast to the bottom of the lower permeability layer, water was steamed in the middle and at the top of the lower permeability layer. Figure 5 shows the steady state steam front extension in the larger (pink lines) and in the smaller (blue lines) tank. Solid lines represent a constant head inflow boundary characterized by a low groundwater flux (below 10 l / (m x d)), whereas dotted lines represent higher discharges (about 333 l / (m x d)).

The cooling effect of increasing groundwater flux had almost no impact on the steam front in the middle of the lower permeability layer (225 cm a.b.) and only a moderate impact on the steam front extension at the top of the aquitard (260 and 295 cm a.b.). In contrast to this the steam front collapsed due to the increased groundwater flux and hot water remained in the center of the lower permeability layer about 40 cm above the aquifer (K_{S2} at 190 cm a.b.) No significant steam front and steam zone were observed at 190 cm a.b. within the relatively higher permeability aquitard material K_{S2}.

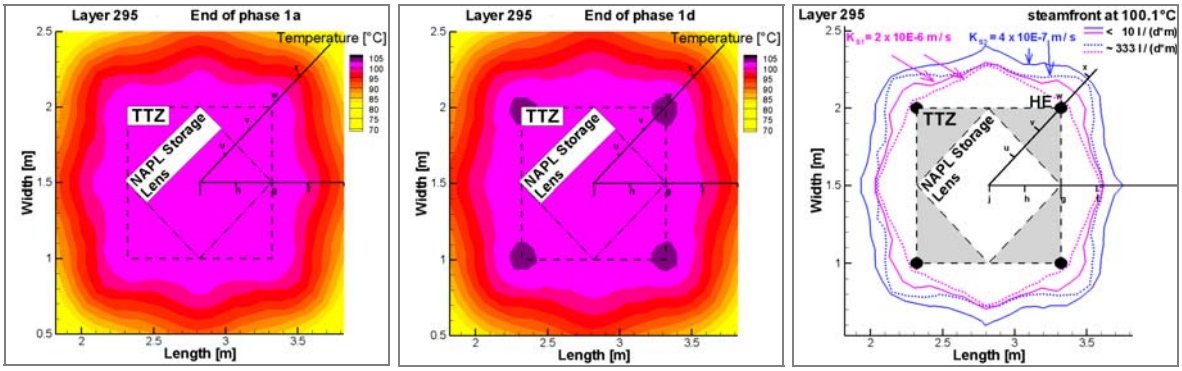

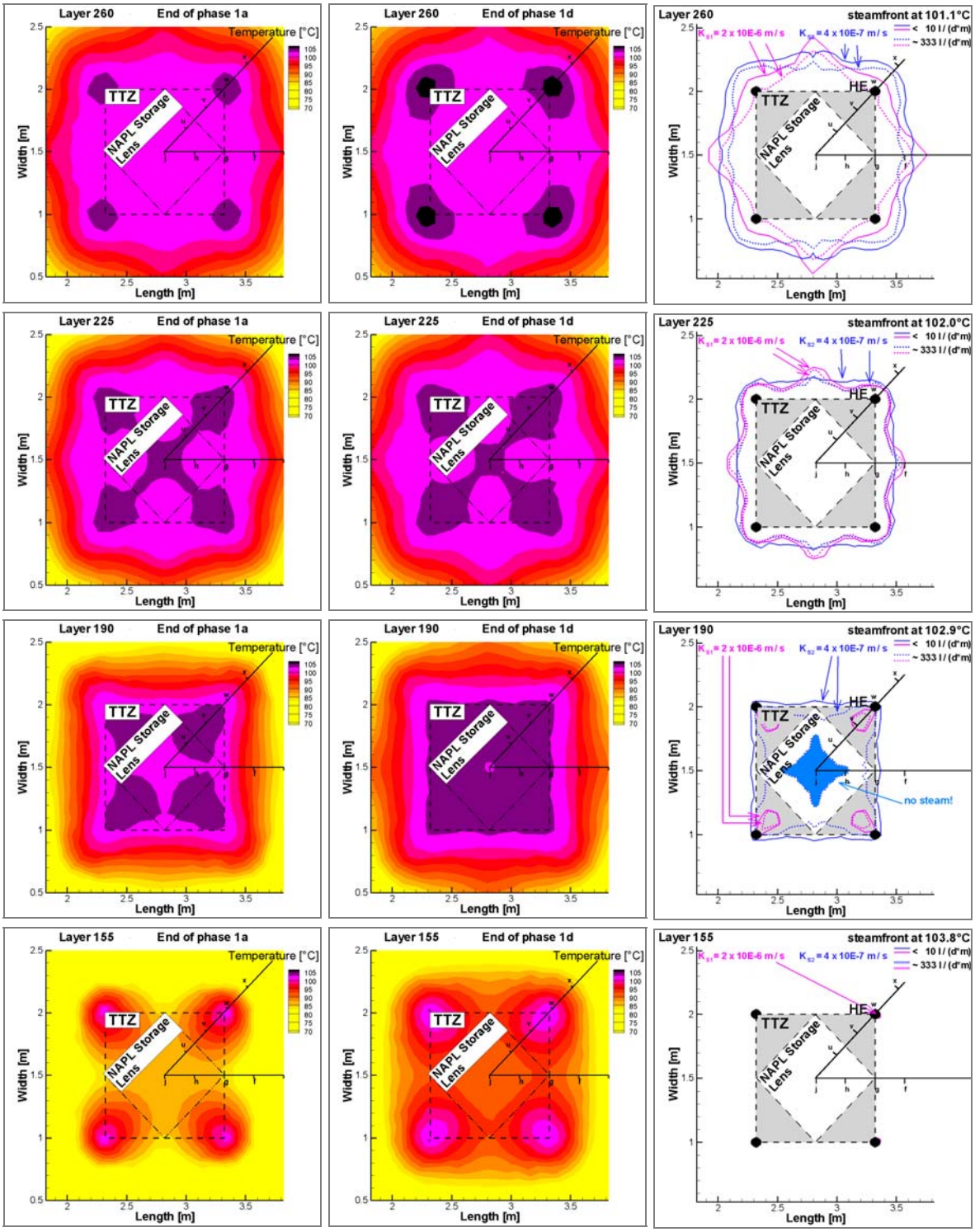

Figure 5: Temperature distribution (left-hand side and middle part) and steam front propagation per measurement layer in both tanks (right hand side, with different permeabilities). TTZ = Target Treatment Zone. Layer 295 was just above the upper DNAPL storage lens, while layer 190 was just beneath the lower DNAPL storage lens.

CONCLUSIONS AND OUTLOOK

An efficient NAPL recovery from the saturated zone by a TCH/ISTD system requires vaporisation of the NAPL and a continuous flow path of the gaseous phase to the unsaturated zone and the SVE wells. Following this approach, the steaming of the water in the aquitard is as important as the formation of a steam override to enable a migration of gaseous NAPL into the unsaturated zone.

The generation of steam by thermal wells is significantly impacted by the soil permeability, hydrostatic pressure dependent on the depth below the groundwater level and, during these experiments, the cooling caused by the groundwater flux (mainly close to the aquifer).

In both heat transfer experiments, in contrast to the numerical forecasts, the achieved temperatures at the bottom of the lower permeability layer (1.55 m a.b.) were not sufficient to produce steam due to the additional hydrostatic pressure of the groundwater at the end of the experiment. Hence, a breakthrough of the steam front from the aquitard into the lower aquifer, as predicted in some numerical simulations for very low ground water flux, was not seen.

Also, with the given heater power of 6 kW, no significant steam production was observed at the bottom of the lower NAPL-storage lens (referring to the measurements at 190 cm a.b = 40 cm above the bottom of the aquitard), with the exception of a groundwater flux of less than 10 l / (m x d) and the lower permeability aquitard. Only in this instance was a circular steam front between the heating elements generated.

In the large tank, the higher permeability of the aquifer increased the groundwater's cooling effect. Thus, steady state temperature conditions were lower than in the small tank experiment with a lower aquifer permeability.

For the given power and arrangement of the heater wells at a spacing of 1 m, a high groundwater flux can limit the downward expansion of the steamed zone. In the case in which NAPL would be located in the lower portion of a water saturated aquitard, contaminant recovery via conductive heating and a SVE-system would be impossible under these conditions. The experimental results indicate the requirement of an advanced numerical simulation to predict the steam front propagation, the temperature distribution and the recovery of NAPL. The data are currently being analysed and compared with advanced numerical simulations.

Remediation experiments are currently under operation in the tanks. Results from these experiments as well as a comparison of experiments and numerical simulations will be discussed during the oral presentation and compared with the results from 2-D experiments [BAKER AT AL. 2008].

ACKNOWLEDGEMENT

This research was supported wholly (or in part) by the U.S. Department of Defense, through the Strategic Environmental Research and Development Program (SERDP).

REFERENCES

BAKER, R. G. HERON, J. LACHANCE, A. FÄRBER, L. YANG, AND U. HIESTER 2008. *2-D physical models of thermal conduction heating for remediation of DNAPL source zones in aquitards.* In *Conference Proceedings: 10th International FZK//TNO Conference on Contaminated Soil (ConSoil 2008)*. 4-6 June, Milan, Italy. http://www.consoil.de.

LI, J. 2004. *Experimental Investigation on Thermally Induced Buoyancy Flow in Porous Media,* Masters Thesis, Universität Stuttgart, Institute of Hydraulic Research, Thesis-supervision Arne M. Färber, Olaf A. Cirpka, Stuttgart, Germany.

WAGNER W.: *New vapour pressure measurements for argon and nitrogen and a new method for establishing rational* vapour *pressure equations*. Cryogenics, 13(8), 470-482, 1973

UDELL, K.S. & FITCH, J.S. 1985. *Heat and Mass Transfer in Capillary Porous Media Considering Vaporisation, Condensation and Non-Condensible Gas Effects*. Paper presented at 23rd ASME/AIChE, *National Heat Transfer Conference*, Denver, CO.